Department of AERONAUTICS and ASTRONAUTICS
STANFORD UNIVERSITY

R. CARLSON
B. SCHNEIDER
L. BERKE

AN EXPERIMENTAL STUDY OF THE CREEP BUCKLING OF CIRCULAR CYLINDRICAL SHELLS UNDER AN AXIALLY APPLIED COMPRESSION

OCTOBER
1965

Technical Report No. 16
Prepared for the Office of Naval Research of the U.S. Navy
Under Contract Nonr-225(30)
Project NR 064-425

SUDAER
NO. 248

Department of Aeronautics and Astronautics
Stanford University
Stanford, California

AN EXPERIMENTAL STUDY OF THE CREEP BUCKLING OF CIRCULAR CYLINDRICAL SHELLS UNDER AN AXIALLY APPLIED COMPRESSION

by

R. Carlson, B. Schneider, and L. Berke

SUDAER No. 248

October 1965

The work here presented was supported by the United States Navy under contract Nonr 225(30) and 225(47) monitored by the Mechanics Branch of the Office of Naval Research

SUMMARY

The use of electroforming to produce circular cylindrical shells is described. Examples are cited for which the use of electroforming provides opportunities for the development of unique specimen designs and test procedures.

The use of a tapered creep specimen to generate isochronous stress-strain curves is described. The procedure developed provides a method for deriving basic creep relationships from data obtained from a small number of tests.

The results of creep buckling tests on circular cylindrical shells under axial compression are presented. The basic features described are the end-shortening history, the variation of buckling load with time, and the post-buckling pattern which is developed.

INTRODUCTION

The fact that solids under load can exhibit time-dependent deformation or creep has been rather common knowledge to engineers for many years. To a large extent, however, creep has been eliminated as a design factor. This has been done by the restriction of operating conditions or, when this has not been possible or desirable, by the development of special, creep resistant materials. In some instances the less satisfactory solution of increasing section size to reduce the operating stress level has been used.

The strategy of avoiding creep as a design factor cannot be expected to continue to provide a satisfactory solution to all structure problems, however. Where extreme operating conditions are encountered and weight is an important factor, an efficient design can be expected to require an analysis which includes a consideration of creep. During the past fifteen years, a number of investigators have realized that creep effects could introduce design problems and considerable research effort has been devoted to studies of creep effects in structures.

In the studies that have been reported one important class of problems involves the possibility of creep induced instability or creep buckling. The usual practice for developing design procedures to account for new phenomena is to first treat simple structural elements under simple loading conditions. Following this procedure, the column has been studied—both experimentally and analytically—and the resulting knowledge of the mechanics of column creep buckling is relatively complete. A thorough survey of investigations of column creep buckling

has been presented by Hoff [1][1] so this material will not be reviewed here.

The results presented in this report are part of a program designed to study the creep buckling of a basic structural element—the axially compressed, circular cylindrical shell. The elastic buckling of this element has been studied quite intensively in the last few years [2,3] and our understanding of the basic phenomenon has been substantially improved. The extension of creep buckling studies to the circular cylinder can now, therefore, be expected to provide meaningful results.

The creep buckling of axially compressed, circular cylinders has been studied by several investigators [4,5,6,7]. Several different methods of analysis have been proposed and limited experimental data have been obtained. The analysis of the problem is difficult and the various simplifications that have been adopted have led to a variety of criteria for the onset of instability. These results, which are essentially exploratory, will be discussed in greater detail in a subsequent report. The amount of experimental data available is quite limited. The results of Gerard and Gilbert [4] are for radius to thickness ratios of 10 to 20, so their shells are relatively thick. The experiments of Samuelson [7] include results from seven buckling tests, but since four different radius to thickness ratios were tested, the variation of buckling load with time is not firmly established. From this brief review it is evident that additional studies are necessary, and that a program which includes both analytical and experimental studies is particularly desirable.

---

[1] Numbers in brackets designate References at the end of the report.

The plan of the present program was to perform both experimental and analytical studies of the creep buckling of axially compressed, circular cylinders. This report provides a description of the experimental phase of the program. Detailed descriptions of the specimen fabrication, the equipment and procedures, and the experimental results are presented in the sections that follow.

EXPERIMENTAL PROGRAM

Selection of Material

The difficulties associated with the fabrication of shell bodies has tended in the past to be a deterrent to experimental studies involving shell structures. When experimental studies were undertaken, investigators usually formed commercially available flat sheets to the desired shape and then, when necessary, connected edges by seams. This procedure has a number of obvious disadvantages, and often it has been concluded that test results obtained have been influenced by a property introduced by the fabrication process.

Several years ago Thompson [8] recognized that the principles of electroplating could be used to electroform shell specimens which were free of many of the disadvantages common to the more customary methods of fabrication. Interest in making shell bodies by electroforming has become well established and several investigators [9,10,11] have used the process to make specimens for shell investigations. The results of these studies indicate that the apparent advantages of the process can be realized and that specimens of good quality can be obtained.

The electroforming process was used in the program described by this report to make circular, cylindrical shell specimens. The arrangement of the plating facility* is shown in Figure 1. A molded, polyethylene tank was used to hold the plating solution. Two emersion type heaters were used to heat the solution and the temperature was controlled to within $\pm 5^{\circ}F$ of $115^{\circ}F$. A filter pump was operated continuously to filter out macroscopic particles and to maintain continuous circulation.

*A more detailed description of the facility is given in Reference 12.

The polyethylene sheeting shown in Figure 1 enclosed the space above the surface of the bath to prevent contamination of the bath by airborne particles.

Nickel was selected for the studies described here because deposits of relatively high strength and, more importantly, high proportional limit stress can be readily obtained. Anodes of rolled, depolarized nickel were used. As can be seen in Figure 1, they were enclosed in bags to prevent the formation of nodular deposits [13].

A sulfamate bath [13] was used and a pH of 4 was maintained. The specific gravity was kept at 1.25 and a current density of 42 amps per sq. ft.—in terms of the surface area of the mandrel being plated—was used. The mandrel was attached to the lower end of the rod above the bath in Figure 1. The rod and the mandrel in the bath were rotated continuously during plating.

The structure of the deposits produced during electroforming is complex and depends on the bath composition and the operating conditions. Also, the structure of the initial deposits can depend on the base metal and may, in some instances, be a continuation of the structure of the base metal [14]. This can occur, for example, if both metals are cubic. In this program the nickel and the aluminum alloy (2024-0) mandrel were both face centered cubic, but the difference in lattice parameter exceeds that for which continuation growth may be expected [14].

When deposits are not constrained to adopt a particular texture, they assume orientations such that a crystal axis is perpendicular to the surface or parallel to the direction of current flow [14]. The orientation with respect to normals to the surface is random. Thus,

the mechanical properties in elements tangent to the surface should be isotropic. Properties in a direction normal to the plated surface would be different from those of elements tangent to the surface.

The primary stresses in the circular cylindrical shells tested in this program act in directions tangent to the mid-surface of the shell wall. From the previous discussion regarding the growth characteristics of nickel deposits, it follows that the shells can be considered to be isotropic; i.e., properties in the direction normal to the shell mid-surface need not be considered.

An examination of the microstructure of samples of the electroformed nickel was made and it was found that the material was sound and free of voids. The microstructure of the as-plated material, which is shown in Figure 2, is typical of the structure which can be obtained for electrodeposited nickel [15]. Fibrous or columnar grains run normal to the surface of plate and in the direction of growth during plating (the view shown is a transverse section through the thickness of the plated sample). The specimen shown was polished and etched for 2 second in a solution containing equal parts of nitric acid and acetic acid.

During the experiments conducted in the program, most of the specimens tested were exposed to temperatures of 650°F for periods up to about 5 hours. The response of the microstructure to such an exposure is, therefore, of interest. Accordingly, a specimen which was heated at 650°F for 5 hours was polished and etched, and the microstructure was examined. No change from the microstructure shown in Figure 2 could be discerned. This observation is in accord with information in the literature [13] which indicates that only minor structural changes

occur in nickel deposits below 1100°F. It is to be noted, however, that some softening can be observed, at 500°F [13], so the exposure at 650°F can be expected to have some effect on the mechanical properties of the deposits. This effect is confirmed in a subsequent section.

To illustrate the change in structure that can occur at temperatures well above 650°F, a sample was heated at 1400°F for 0.75 hour. The microstructure of this sample is shown in Figure 3. The grain growth which is apparent is typical of the response to be expected for nickel deposits exposed to this heat treatment [15]. The same etching procedure used for the sample of Figure 2 was utilized.

Mechanical Properties

An analysis of the creep buckling of axially compressed, circular cylindrical shells must make use of laws governing the elastic and the creep response of the shell material. In this program the tensile test was used to obtain Young's Modulus and the simple torsional pendulum was used to obtain the modulus of rigidity. A special test was devised to obtain the creep properties of the shell material. The procedures of testing and the test results for each of the above properties are presented in the sections which follow.

The Tensile Test

The tensile properties were determined by conducting tensile tests on samples cut from shells plated on the octagonal mandrel on the right in Figure 4. Both the octagonal mandrel and the circular mandrel (on the left) which was used to make the cylindrical shells were machined

from stock of about the same size. The approximate equality of size and surface area made it possible to use essentially the same plating conditions with both mandrels. The flat surfaces plated on the octagonal mandrel, however, provided blanks which were easy to prepare for tensile testing.

Blanks cut from the octagonal shell were placed in templates, cut to the desired size, and drilled at the ends to receive centering pins for clamp-type loading shackles. The tensile specimens were 2.25 inches long, 0.3 inch wide and 3.0×10^{-3} inch thick.

The specimens were prepared for testing by applying a Type AF-7-1 wire resistance strain gage to each face. The strain readings were obtained by the use of an SR-4 Strain Indicator. The load was applied directly in increments of about 5 pounds and the Indicator readings and load values were converted to strain and stress values.

Stress-strain curves for typical results are presented in Figures 5 and 6. The curve of Figure 5 represents the tensile properties of the nickel in the as-plated condition.

Prior to the application of the load in the creep buckling tests, specimens are heated from room temperature to 650°F in about five hours. The specimens are then held at 650°F for one half hour before the load is applied. As noted in the section Selection of Material, this exposure can be expected to result in some softening of the material. The stress-strain curve for a specimen exposed to the above temperature history is presented in Figure 6. A comparison of Figure 5 and 6 indicates that softening does occur for this exposure. A tabulation of the tensile properties for the two conditions is given below.

Condition	Young's Modulus (10^6 psi)	Proportional Limit Stress (10^3 psi)	0.1 Per Cent Offset Yield Strength (10^3 psi)
as-plated	25	17	50
heat treated	27	14.5	40

Note that the indices of the resistance to plastic flow have been decreased by the heat treatment.

It is of interest to note that the heat treatment produces a slight increase in the value of Young's Modulus. This is not a spurious result. In fact the trend is repeated with the modulus of rigidity measurements. The behavior observed is related to an interaction of stress and magnetostrictive effects which can, for example, cause the observed modulus of nickel to change with the application of a magnetic field [16,17]. Heat treatment can also modify internal magnetic structure and result in a change in the response of the nickel to externally applied stresses [17].

The Torsional Pendulum

Modulus of rigidity values from room temperature to 650°F were determined by the use of a simple torsional pendulum. Two cylindrical steel bars which had clamps at one end were made to grip a strip specimen of nickel. One of the bars was bolted to the top cover of a tube type furnace. The lower steel bar served as the rotating inertia mass or pendulum bob. By positioning the assembly in a furnace, readings could be taken as the temperature was slowly increased.

The stiffness of the nickel strip, which had a rectangular cross-section, was computed from results available in the theory of elasticity

for torsion of non-circular cross-sections [18]. The rigidity modulus, G , can then be computed by the use of the equation

$$G = \frac{12\pi^2 LJf^2}{t^3 b(1-0.63\ t/b)} \quad , \qquad (1)$$

where

L is the strip length,

J is the mass moment of inertia of the pendulum bob,

f is the frequency of oscillation,

t is the thickness of the strip,

and b is the width of the strip.

Specimens were cut from nickel plated octagonal shells (see the octagonal mandrel in Figure 4) and trimmed to provide the following strip dimensions:

L = 4.00 inches,

t = 0.0033 inch,

b = 0.254 inch.

The value of $J = 6.98 \times 10^{-4}$ lb. sec^2 inch.

The quantity determined from the tests was the period of oscillation. This was obtained by measuring the time-by stop watch-required for 70 cycles to occur. Small amplitudes were used and the extremes were easily noted by observing a reflection from a small mirror attached to the pendulum bob. The time for 70 cycles could be repeated to within less than one half of one per cent.

In the previous section on tensile properties the effect of exposure to elevated temperature on the room temperature value of Young's Modulus

was noted. In the tests on the torsional pendulum it was possible observe the effect on the elastic response as the temperature exposure occurred. The variation of the rigidity modulus with temperature for two heating cycles is shown in Figure 7. The total time required to increase the temperature to 650°F was about 8 hours.

Data for the first test are plotted as circles—open and solid—and they represent the response of the material in the as-plated condition. Data for the second test are plotted as squares—open and solid—and they represent the response of the nickel plate after exposure to elevated temperatures up to 650°F. The cross represents the end of the first test and the beginning and end of the second test. Note that the data for heating and cooling for the second test lie on the same curve. Note also that the data for cooling for the first test also lie on the curve obtained for the second test. This indicates that the modulus of rigidity stabilized at a new value. Since the tests conducted on the circular cylindrical shells involve heating to and soaking at 650°F, the stabilized elastic response indicated by the curve for the second test should be used in analyses of creep buckling experiments.

Creep Properties

The creep buckling tests on the circular cylinders were conducted at 650°F and at average stress values from 7,000 psi to 10,000 psi. This stress-temperature environment resulted in collapse of the cylinders in times up to about 200 minutes. The creep data necessary to perform an analysis of the cylinder buckling tests were obtained by testing specially designed tensile specimens at 650°F at stress levels, and for time periods

such that the range of interest was covered.

Because the specimens were very thin, standard methods of creep testing and strain measurement were not attractive. Instead of carrying out a large number of creep tests on standard tensile specimens, a slightly tapered test specimen* was designed. Then, one test could cover a range of stress values and provide enough data for deriving an isochronous stress-strain curve for the stress range of interest.

The geometry of the test specimens and the location of the gage section are shown in Figure 8. The location of the gage section was selected after a stress analysis using the method and computer program of Ref. 20. In the analysis the specimen was considered clamped at the ends of the reduced section. The length and location of the test section within the reduced section was selected such that the deviation from the average stress at each section was less than one per cent.

To obtain flat specimens and yet to have a plating process as similar to that for the circular cylinders as possible, octagonal cylinders were plated to the same thickness and in the same bath. Each octagonal cylinder provided eight flat blanks (0.96 x 5.0 in.) after being filed apart at the edges.

To obtain uniform geometry of the test specimens, two hardened steel templates were made such that their use also ensured symmetry of the specimens. The templates are shown in Figure 9. In making a specimen a plated blank was clamped between the templates which were positioned

*After the use of the tapered specimen was introduced in this program, Levy and Barody published a paper [19] on such a specimen. Their method of processing data is different, however.

using the outer two holes. The specimen centering holes were then drilled and reamed using the two inner holes. After putting 1/4 inch pins in these holes, one half of the specimen was cut to size. Next, the specimen was turned around, secured again with the pins, and the other side was cut to size. In the last operation made the test section was marked to provide markings for reading distances under a microscope. One of the hardened templates was marked by the desired eleven markings 4mm apart giving a test section of 40 mm. Securing the test specimen once more with the pins in this template, and using a steel ruler and a needle sharpened under a microscope, the eleven markings were lightly scratched on the specimen. This operation prepared the specimen for reading and testing.

A small surface irregularity adjacent to each of the eleven scratches was used as a reference point. The reference points selected were much smaller than the scratches and permitted a significant improvement in reading reproducibility. By the procedure used, the scratches served two functions. First, they provided a means for obtaining the desired spacing of the reference points. Second, they were useful in identifying the reference points. This latter function was facilitated by the use of a sketch of the microscopic field of each reference point and its adjacent scratch.

Creep strains were obtained by measuring the relative position of the eleven stations in the test section before and after creep testing. The difference in the position of the two sets of these data were plotted versus the station location before creep. The curve through these points represents displacement relative to the first station. The slope

represents the local strain.

Measurements were made with a Hilger and Watts comparator microscope. Reproducibility of the readings was $\pm$ 0.001 mm. To obtain the cross-sectional dimensions at the eleven cross sections thesame microscope was used to measure the widths and a micrometer with a vernier was used to measure the thicknesses. The thicknesses were found, for specimens cut from the same cylinder, to be the same to within $\pm$ 0.0001 in.

The load applied to the specimens was 13.47 lbs. for all tests. Using the measured cross-section area at the eleven markings and the applied load, eleven stresses were calculated for each specimen and plotted against the strains measured at the same markings. The times used for the tests were selected to cover the same range as the cylinder creep buckling times. They were: 24, 48, 96, and 192 minutes. Thus each series of tests gave four isochronous stress-strain curves that covered the required stress and time range at 650°F . Each test involved the use of one blank from an octagonal shell; thus for the four times above, four specimens were used.

A furnace similar to the one used for the creep buckling tests was used to conduct tensile creep tests. The same unit was used to control the test temperature. The details of the temperature control unit are presented in a subsequent section.

The loading fixtures consisted of a pair of hardened grips clamped to each end of the specimen, and universal type clevis connections which transferred the load to the end grips through hardened pins. Because the specimen cross-section was small, the level of stress required was easily attained by applying weights to a loading pan suspended from the

lower clevis.

To avoid creep recovery effects, the specimen was removed from the furnace with the load on. The load was not removed until the specimen had cooled to room temperature. Displacement readings taken immediately after the test were repeated after a lapse of 24 hours and no significant difference in values could be detected. This observation, which indicates that creep recovery did not influence the results, agrees with results obtained by Levy and Barody [19].

The tests and the measurements obtained gave isochronous stress-strain curves after a graphical differentiation to obtain the strain. The method used in generating the test data resulted in very little scatter of the test points.

As an illustration of the method of reducing the data, the results for one octagonal shell will be presented. The creep displacements relative to the narrow end of the specimens for times of 24, 48, 96 and 192 minutes are plotted in Figure 10. The load for each time was 13.47 lbs. The slopes of the curves of Figure 10 are plotted against their respective stations in Figure 11. The values of the slopes provide the creep strain gradient along the tapered specimens. The values of the stresses at each station can be readily computed* so the curves of Figure 11 can be easily converted to isochronous stress-strain curves for the times of 24, 48, 96 and 192 minutes shown in Figure 12. The usual plot of creep strain versus time can be obtained from Figure 12 and results are presented in Figure 13 for six values of stress.

*The strains are small so the original specimen dimensions can be used.

The creep data described above were obtained to provide a means for determining an appropriate creep law for the electrolytically deposited nickel. The total number of shells tested in the creep buckling program was thirteen. The octagonal shell discussed above was plated near the beginning of the circular shell production. A second octagonal shell was plated near the end of the circular shell production. The creep data obtained from the second specimen closely reproduced that obtained from the first, so it can be deduced that the plating process produced specimens with uniform properties.

An analysis of the creep data obtained indicated that a creep law of the form

$$\epsilon = \left(\frac{\sigma}{\lambda}\right)^{m} \left(\frac{t}{\tau}\right)^{1/n} \qquad (2)$$

is appropriate. In this relation ϵ is the creep strain σ is the stress in psi., t is the time in minutes, and the constants have the following values:

τ = 1 minute,

$\lambda = 3.24 \times 10^{5}$ psi.,

$m = 2.4$,

$n = 2$.

This law will be used in an analysis of the creep buckling results.

Creep Buckling Experiments

Specimens

Circular cylindrical shells were electroformed on the aluminum alloy mandrel on the left in Figure 4. A typical plated specimen, ready for

testing, is shown on the left in Figure 14. The process of electroforming and the basic properties of the deposited material have been described in preceding sections.

Usually, cylindrical shells which are to be tested in compression are prepared for testing by embedding the free edges in end caps to reinforce the edges against local buckling. For creep buckling tests, however, this method of specimen preparation introduces problems. Prior to the application of the compressive load in the creep buckling tests, the specimen temperature has to be increased. In this program an increase of about 570°F was necessary. With a specimen assembly consisting of several parts attached together, it would be, with this temperature increase, difficult to avoid the introduction of restraining forces at the free edges as the parts expanded.

The need for increased stiffness at the edges without the problems of relative expansion of an assembly was satisfied by producing specimens which had a uniform thickness in a central region and a build-up of thickness at the ends. Thus, during the heating period, prior to the application of load, the specimen was free to expand.

The build-up in thickness desired was obtained by capping the mandrel on the left in Figure 4 with plexiglas disks. The mandrel had a diameter of 2.45 inches and the disks used had a diameter of 2.58 inches. This assembly, when lowered into the plating bath and rotated about its axis, provided specimens of the desired type. A description of the thickness along an element of a typical specimen is given in Figure 15. The specimen on the right in Figure 14 illustrates the type of buckle pattern formed in the creep buckling tests. Note that a two tier

buckle pattern has been developed and that there is no evidence of edge buckling.

After plating, the mandrel was cooled quickly, and the shell specimen was slipped off. Prior to testing, the thickness was measured along four elements of the cylinder. The elements were located at 90 degree intervals along the circumference. Thickness measurement transverses of the type shown in Figure 15 were made with a dial gage jig. The smallest indicated reading was 0.0001 inch.

The thickness of most of the specimens in the central region was about 0.0032 inch. The inside diameter of the cylinders was 2.45 inches and the overall length was 4.5 inches.

Equipment

The loading unit developed for the creep buckling tests was of the lever-arm, dead-weight type. Two views of the unit are shown in the photographs of Figures 16 and 17.

Load was transmitted from the loading pan to the lever arm through knife edge supports. The lever arm rotated about a rod passing through ball bearings housed in two pillow blocks. The rod applying the load to the specimen was guided by two linear bearings and the force was transmitted to it from the lever arm through a hardened steel, double knife-edge. The unit was calibrated and found to have an effective lever-arm of 7.32.

When buckling occurs, a buckle pattern develops and the buckle depth depends on the force transmission characteristics of the testing unit. For a dead-weight or soft system of the type used, the continued

application of force would crush the specimen and the pattern developed upon buckling would be badly distorted. To prevent this distrotion of the pattern, a cylinder, shorter and smaller in diameter than the specimen, was centered on the loading pad. This cylinder limited the amount of end shortening and helped to preserve the post-buckle pattern. No restriction to lateral displacement was exerted by the stop device as its diameter was substantially less than that of the test specimen.

The split-furnace used is shown in Figures 16 and 17. Each half of the furnace contained two semi-circular electrical resistance heating elements. The four heating elements were wired in series, but an external shunt was placed across the two upper heating elements to provide for a uniform temperature distribution. The furnace was balanced by embedding a total of twelve thermocouples in the wall of a shell specimen. The temperature distribution along the length around the circumference was obtained, and at the test temperature of 650°F, the variation from 650°F was less than $\pm$ 4°F. The control thermocouple, which pressed against the surface of the specimen as shown in Figure 17, was calibrated against the embedded thermocouples to provide for a corrected control temperature.

The output of a thyratron power control unit with a 210v input was adjusted to provide the desired level of power to the furnace. The input to the furnace was controlled by the use of a switching circuit actuated by a Leeds-Northrop Micromax Indicating Controller. The output from the control thermocouple was monitored by the controller. Power to the furnace was increased or decreased when the temperature was, respectively, low or high. The temperature was recorded continuously and the variation with time was less than $\pm$ 3°F from the test temperature.

End-shortening of the shell specimen was obtained by measuring the displacement of the lever arm with a dial gage whose smallest indicated reading was 0.001 inch. The dial gage can be seen in Figure 16.

Test Procedure

Prior to testing, the thickness of each specimen was measured. The test specimen was then centered on the loading pad of the loading unit (see Figure 16). The furnace was then closed and the specimen was heated to the test temperature of 650°F in about 5 hours. After stabilizing at the test temperature for 30 minutes, a preselected load was applied to the loading pan. The load pan was then lowered onto the lever-arm. As noted previously, the temperature was controlled and recorded during the test. End-shortening readings were taken frequently to provide an end-shortening versus time curve. The test was terminated when buckling occurred. Buckling was easily detected as there was a sudden drop in the lever-arm at the loading pan end. The drop in the arm was interrupted by the stop device positioned inside of the specimen.

Test Results

The data obtained from the creep buckling tests on circular cylindrical shells under axially applied compression are presented in Table 1. All of the data are for tests conducted at 650°F. The time at which buckling occurred has been designated as the failure time.

No attempt was made to obtain data for zero-time buckling because in creep buckling tests, such results are strongly affected by the rate at which the load is applied. Two zero-time buckling tests were, however,

conducted to determine the room temperature buckling load of the shells produced in this investigation. Specimens number 44 and 49 were used for this purpose and the results are tabulated below:

Specimen No.	Percent of Theoretical*
44	51
49	60

* $100 \times \frac{\text{Experimental Buckling Stress}}{\text{Classical Buckling Stress}}$

These results indicate that the test specimens are of relatively good quality. It has only been rather recently, in fact, that results significantly better have been obtained [2].

The results of the creep buckling tests are discussed in the next section.

TABLE 1. CREEP BUCKLING TEST RESULTS

Specimen No.	R*/h	Average Stress (10^3 psi.)	Failure Time (minutes)
32	380	8.75	37
35	380	8.25	55
38	380	8.75	44
39	390	8.25	93
40	390	7.45	132
41	380	8.25	48
43	390	9.00	30
45	380	7.45	130
46	390	7.00	186
47	380	9.25	57
48	380	9.75	6

*Radius to thickness ratio

DISCUSSION OF RESULTS

It has been demonstrated in this study that the production of shell specimens by the electroforming process has a number of advantages which are not characteristic of other shell fabrication methods. Small specimens, free of seams are easily produced. Thickness control can be exercised to produce specimens which do not require special mounting techniques. Each of these advantages provides for simplifications of the experimental procedures.

The plating of mechanical property specimens on an octagonal mandrel is a good example of the potential benefits to be gained by the use of electroforming. Plating conditions for the circular, cylindrical mandrel and the octagonal mandrel can be made to be the same. The flat specimen blanks from the octagonal mandrel, however, provide for considerably greater freedom of specimen design than would be possible for blanks taken from circular cylindrical shells. The tapered creep specimen, for example, could not be readily made from a blank with a curved surface.

The introduction of the tapered creep specimen permits the use of relatively simple testing and measurement procedures, and a large amount of data can be generated from a small number of tests. The data obtained can be readily processed to provide isochronous stress-strain curves from which a creep strain relationship for the test material can be derived. A detailed description of this method of obtaining basis creep data is presented in the section—Mechanical Properties.

Data for the creep buckling tests conducted on circular cylindrical shells are summarized in Table 1. For each test an end-shortening

versus time curve was plotted and all curves exhibited the characteristics shown in Figure 18. Note that for the initial part of the curve, after the application of the compressive load, the rate of end-shortening with respect to time decreases with increasing time. Ultimately, there is an inflection point so that thereafter, the rate of end-shortening increases with increasing time. Just prior to buckling, the end-shortening velocity increases rapidly.

The behavior described above is of special interest because a similar response has been observed by several investigators [21,22,23,24] who have conducted experimental studies of column creep buckling. In the column studies, the lateral deflection was recorded but the amplification or growth characteristics were the same as those exhibited in the test result of Figure 18. This behavior is apparently common for metallic structures subject to creep buckling. It can be shown to be related to the capacity of metals to strain-harden during an initial period after loading [25], and it is manifested as the primary stage in a constant stress test. The capacity to strain-harden decreases gradually, however, and then the structural tendency for stress amplification to increase, due to bending, becomes dominant, and the end-shortening velocity begins to increase. A more detailed discussion of this mechanism is presented in a recent report [25].

The data of Table 1 are presented graphically in Figure 19 in the form of an average stress versus failure time plot. Although there is some of the scatter which is typical of creep buckling data, a definite trend is indicated and a curve which gives a good representation of most of the data can be drawn.

No attempt has been made to extrapolate the curve of Figure 19 to zero-time. For times less than the shortest test time of 6 minutes the curve should rise rapidly. If a computation based on the buckling load* given in the previous section is made, however, the zero-time buckling load at 650°F should be of the order of 20,000 psi. If this estimate is approximately correct, it would follow from Figure 19 that there is a drastic decrease in the buckling load due to creep effects. This pattern of behavior is not uncommon in creep buckling. A more thorough evaluation of these results will be presented in a subsequent report in which the method of analysis developed in Reference 25 will be used to compute the variation of buckling load with time.

As noted previously (see Figure 14), a two tier, diamond buckle pattern was developed in the creep buckling tests. The number of dimples formed around the circumference was counted after each test. The number of dimples ranged from 7 to 9 with 8 being a good average. No consistent change in number with failure time could be detected. It is interesting to note, however, that the room temperature, zero-time test specimens had from 10 to 12 dimples around the circumference. The latter result is derived from only two tests, however, so the observed difference in dimple size is not as well substantiated as would be desirable.

*The zero-time, room temperature buckling load was 50 to 60 percent of the classical value.

CONCLUSION

It has been demonstrated that the process of electroforming can be used to produce circular cylindrical shells of good quality. The process has a flexibility which is not common to other methods of shell body fabircation. In the investigation described in this report the use of electroforming provided opportunities for the development of unique specimen designs and test procedures.

The tapered creep specimen can be used to generate isochronous stress-strain curves which can be used as a basis for deriving basic creep relationships. The method developed permits the use of simple testing and measurement techniques and a large amount of data can be generated from a small number of tests.

The behavior of a compressively loaded, circular cylindrical shell which is subject to creep has some features which are similar to those which have been observed for columns subject to creep. In both of these structures the growth or amplification of the measured displacement follows the same pattern; i.e., during an initial period, the displacement velocity decreases with time up to a minimum value, and then increases with time until buckling occurs. Buckling occurs suddenly and the structure essentially loses its ability to support its load as a two tier, diamond buckle pattern develops. The pattern developed is similar in appearance to that obtained in zero-time, conventional tests. The decrease in buckling load due to creep effects is substantial for nickel cylinders at 650°F.

ACKNOWLEDGEMENT

The authors acknowledge the encouragement and helpful comments of Dr. Nicholas J. Hoff, and the diligence of R. L. Sendelbeck who manufactured the test specimens.

REFERENCES

1. Hoff, N. J., "A Survey of the Theories of Creep Buckling", Proceedings of the Third U. S. National Congress of Applied Mechanics, Amer. Soc. Mech. Engr., 1958, p. 29.

2. Almroth, B. O., Holmes, A. M. C. and Brush, D. O., "An Experimental Study of the Buckling of Cylinders Under Axial Compression", Jour. of Experimental Mechanics, Sept. 1964, p. 263.

3. Hoff, N. J. and Rehfield, L. W., "Buckling of Axially Compressed Circular Cylindrical Shells at Stresses Smaller than the Classical Value", Journal of Applied Mechanics, Vol. 32, Series E, No. 3, Sept. 1965, p. 542.

4. Gerard, G. and Gilbert, A. C., "A Critical Strain Approach to Creep Buckling of Plates and Shells", Journal of Aero. Sci., Vol. 25, No. 7, 1958, p. 429.

5. French, F. W. and Patel, S. A., "Creep Buckling of Cylindrical Shells Subjected to Uniform Axial Compression", PIBAL Report No. 489, 1959.

6. Samuelson, A., "An Experimental Investigation of Creep Buckling of Circular Cylindrical Shells Subjected to Axial Compression", The Aeronautical Research Institute of Sweden, Report No. 98, 1964.

7. Samuelson, A., "A Theoretical Investigation of Creep Deformation and Buckling of a Circular Cylindrical Shell under Axial Compression and Internal Pressure", The Aeronautical Research Institute of Sweden, Report No. 100, 1964.

8. Thompson, J. M. T., "Making of Thin Metal Shells for Model Stress Analysis", Journal of Mech. Engr. Sciences, Vol. 2, No. 2, 1960, p. 105.

9. Babcock, C. D., "The Buckling of Cylindrical Shells with an Initial Imperfection under Axial Compression Loading", Ph.D. Thesis, California Institute of Technology, 1962.

10. Parmerter, R. R., "The Buckling of Clamped Shallow Spherical Shells Under Uniform Pressure", Graduate Aeronautical Laboratories, Report SM 63-53, California Institute of Technology, November 1963.

11. Almroth, B. O., Holmes, A. M. C. and Brush, D. O., "An Experimental Study of the Buckling of Cylinders under Axial Compression", Jour. of Experimental Mechanics, Sept. 1964, p. 263.

12. Sendelbeck, R. L., "The Manufacture of Thin Shells by the Electroforming Process", SUDAER Report No. 185 of Stanford University, April 1964.

13. Metals Handbook, Vol. 2, Heat Treating, Cleaning and Finishing, American Society for Metals, 1964, p. 432-443.

14. Barrett, C. S., Structure of Metals, McGraw-Hill Book Company, New York, 1952, p. 513.

15. Blum, W. A., "Properties of Electrodeposited Nickel", Materials and Methods, April 1953.

16. Metals Handbook, Vol. 1, Properties and Selection of Metals, American Society for Metals, 1961, p. 1218.

17. Cochardt, A., "Magnetomechanical Damping", Chapter II of Magnetic Properties of Metals and Alloys, Edited by R. M. Bozarth, American Society for Metals, 1959, p. 253.

18. Timoshenko, S., Theory of Elasticity, McGraw-Hill Book Co., 1934, p. 256.

19. Levy, J. C. and Barody, I. I., "A Set of Creep Curves from a Single Test Using a Tapered Specimen", Journal of the Mechanical Engr. Sciences, Sept. 1964, p. 236.

20. Przemieniecki, J. S. and Berke, L., "Digital Computer Program for the Analysis of Aerospace Structures by the Matrix Displacement Method", Flight Dynamics Lab., Wright-Patterson Air Force Base, TDR 64-18.

21. Jackson, L. R. et. al., "Atress-Strain-Time Properties of Some Aircraft Materials", Weight-Strength Analysis of Aircraft, McGraw-Hill Book Co., New York, 1952, p. 320.

22. Carlson, R. L. and Schwope, A. D., "An Experimental Investigation of the Creep Properties of Aluminum at Elevated Temperatures", Proc. First Midwestern Conference of Solid Mechanics, 1953, p. 180.

23. Mathauser, E. E. and Brooks, W. A., "An Investigation of the Creep Lifetime of 75S-T6 Aluminum Alloy Columns", NACA TN 3204, 1954, p. 18.

24. Webster, G. A. and Alexander, J. M., "An Investigation of Small-deflection Creep Buckling", Joint Internation Conference on Creep, Inst. Mech. Engr., London, Session 2, 1963, p. 18.

25. Carlson, R. L., "Structural Instability Induced by Creep", SUDAER Report No. 244 of Stanford University, Sept. 1965.

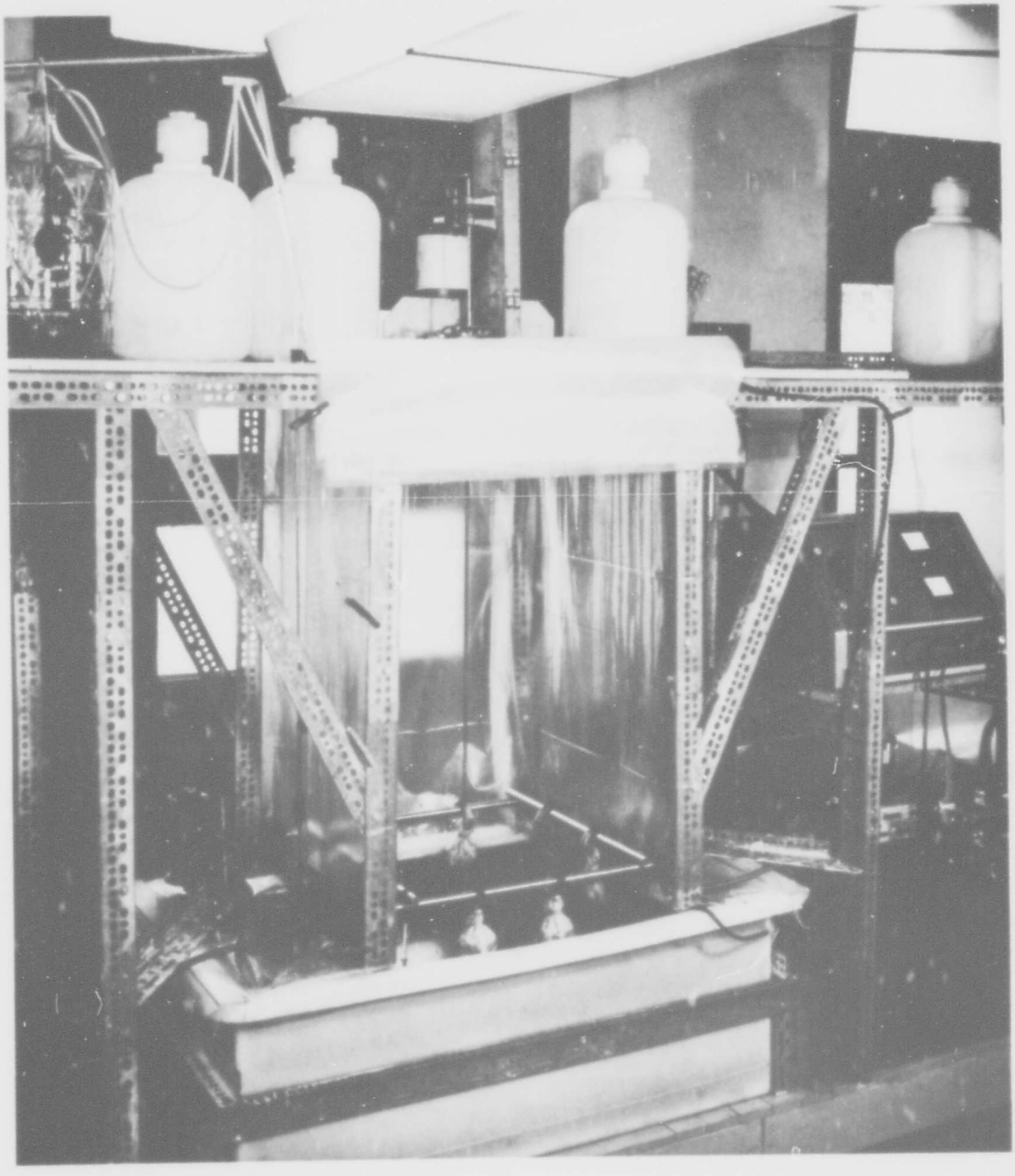

Fig. 1 Electroforming facility.

400X

Fig. 2 As-plated microstructure.

400X

Fig. 3. Fig. 3 Heat-treated microstructure.

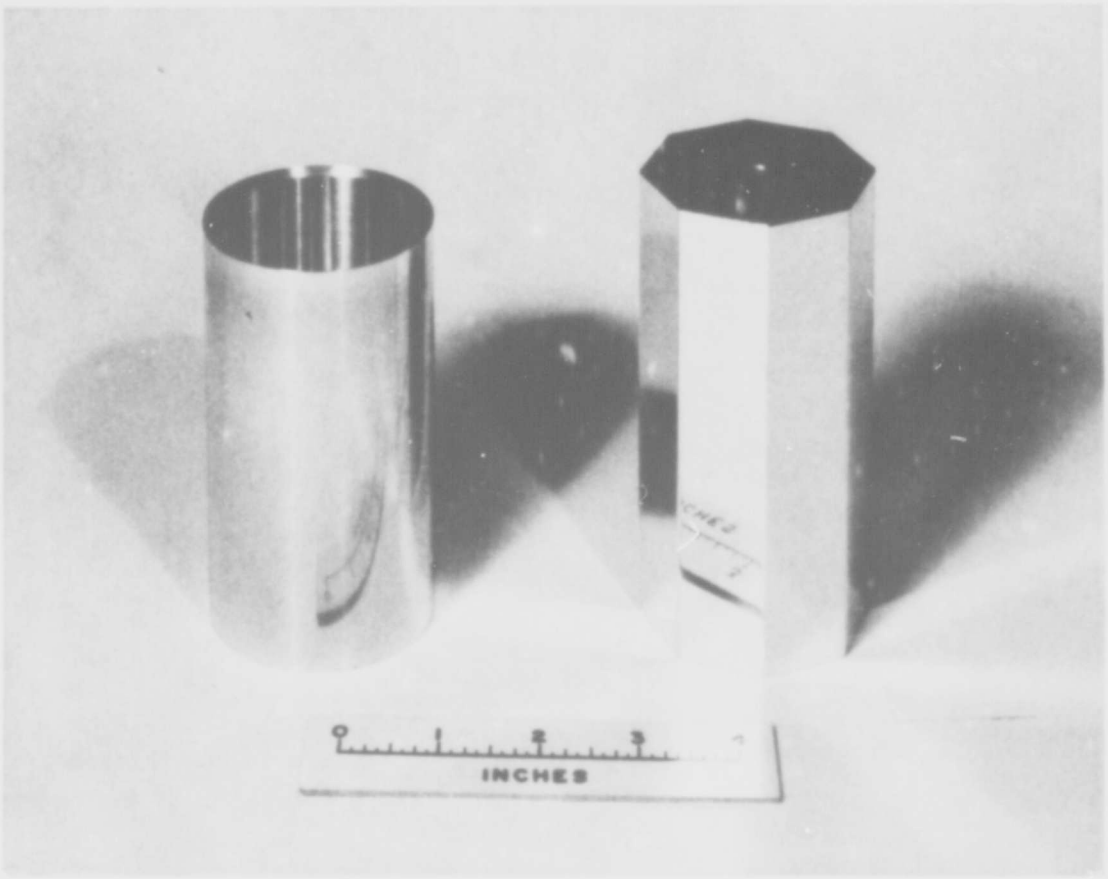

Fig. 4 Mandrels for electroforming shell specimens.

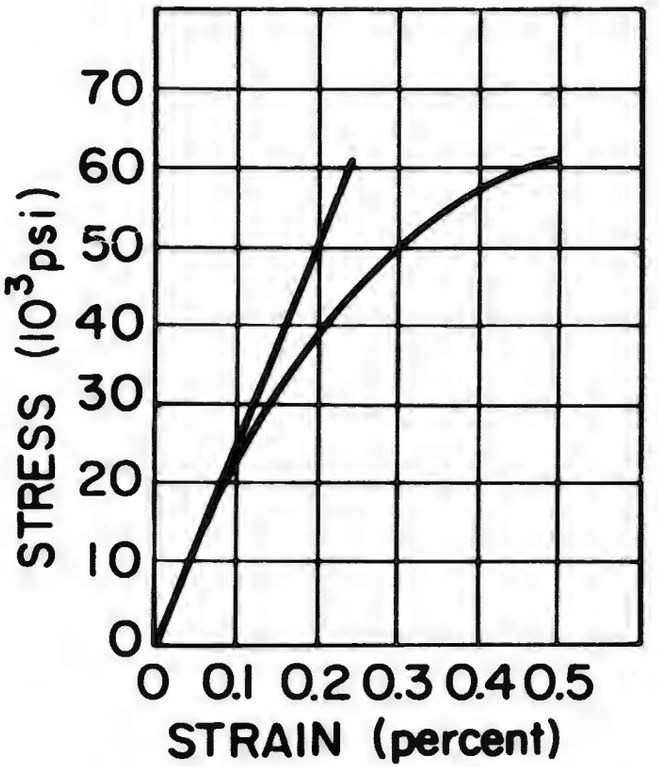

Fig. 5 Nickel specimen, as plated.

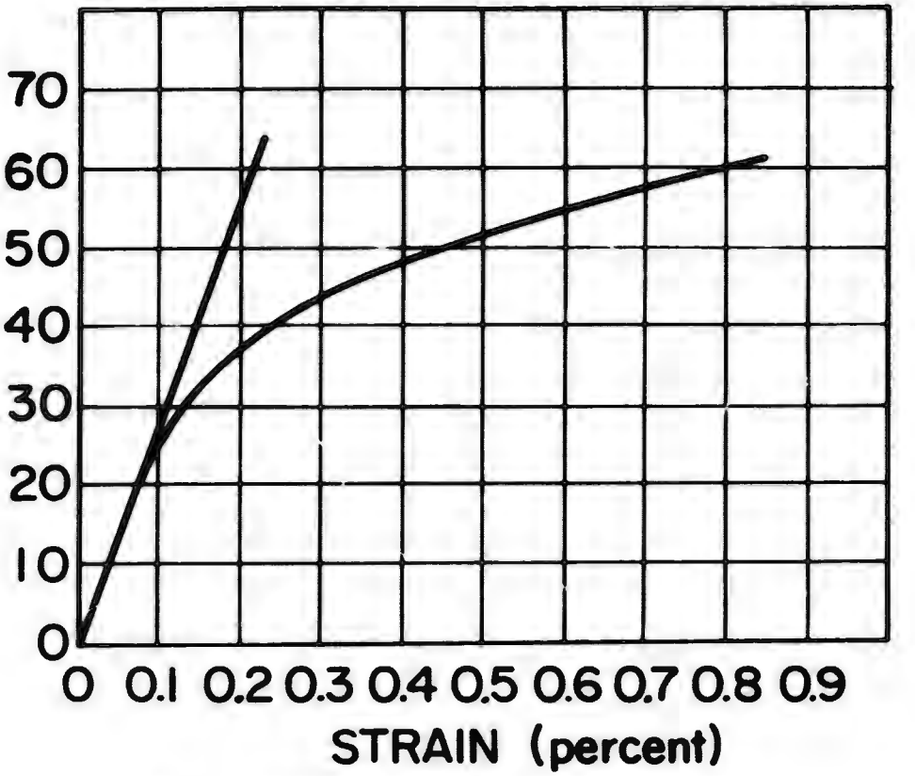

Fig. 6 Heat treated nickel specimen.

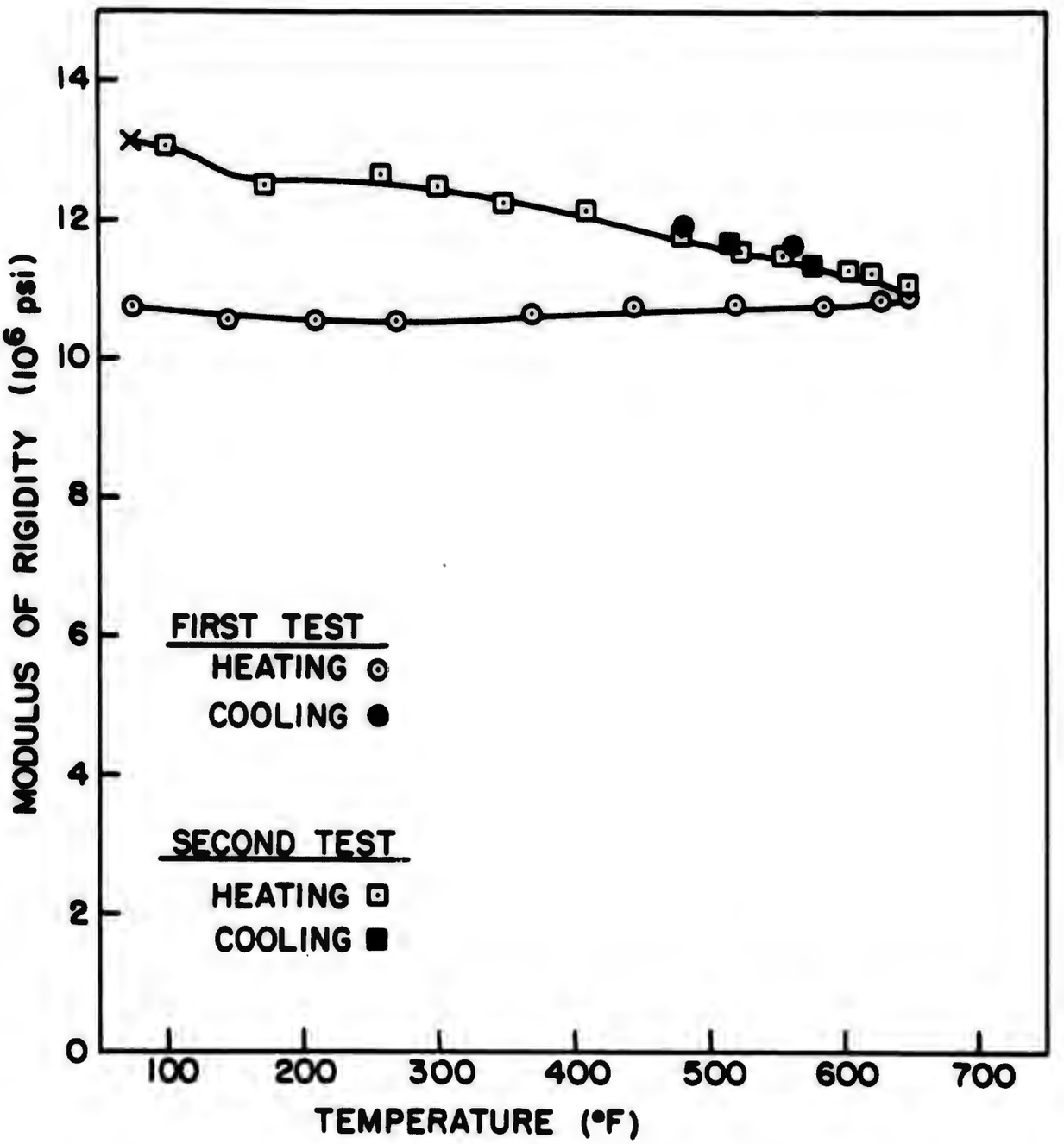

Fig. 7 Modulus of rigidity versus temperature for electrolytically deposited nickel.

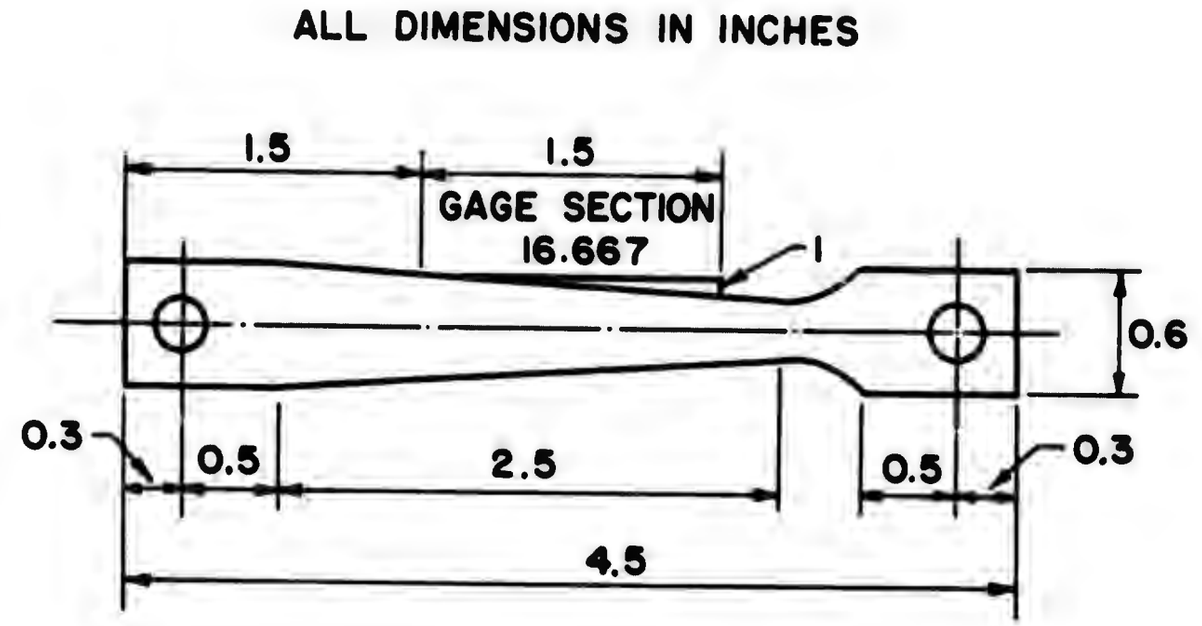

Fig. 8 Tapered specimen.

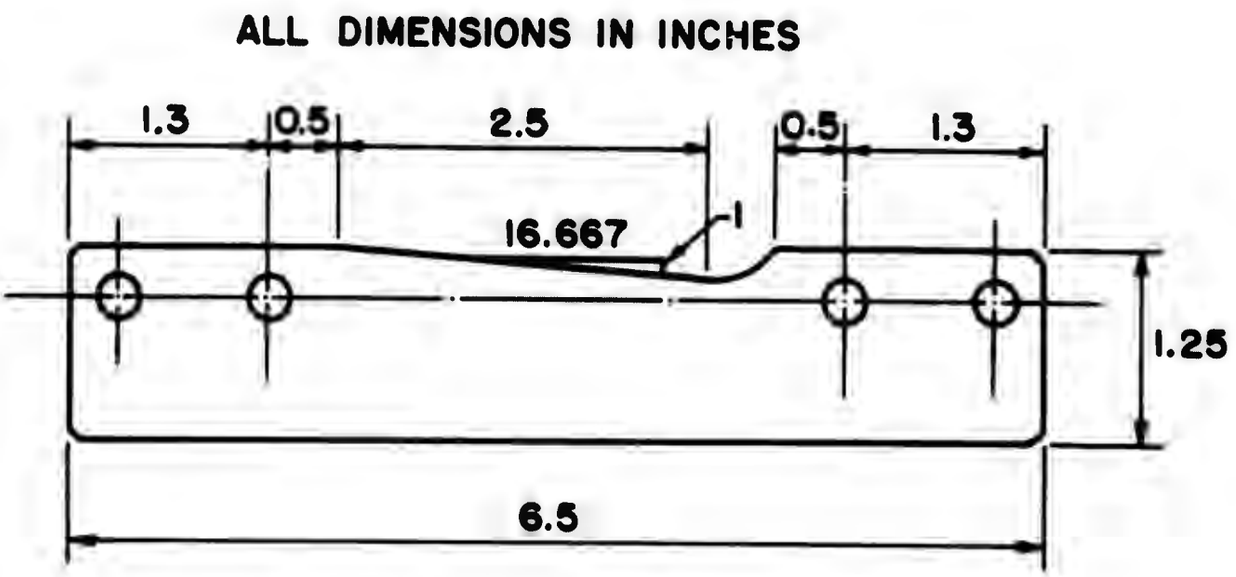

Fig. 9 Template for tapered specimen.

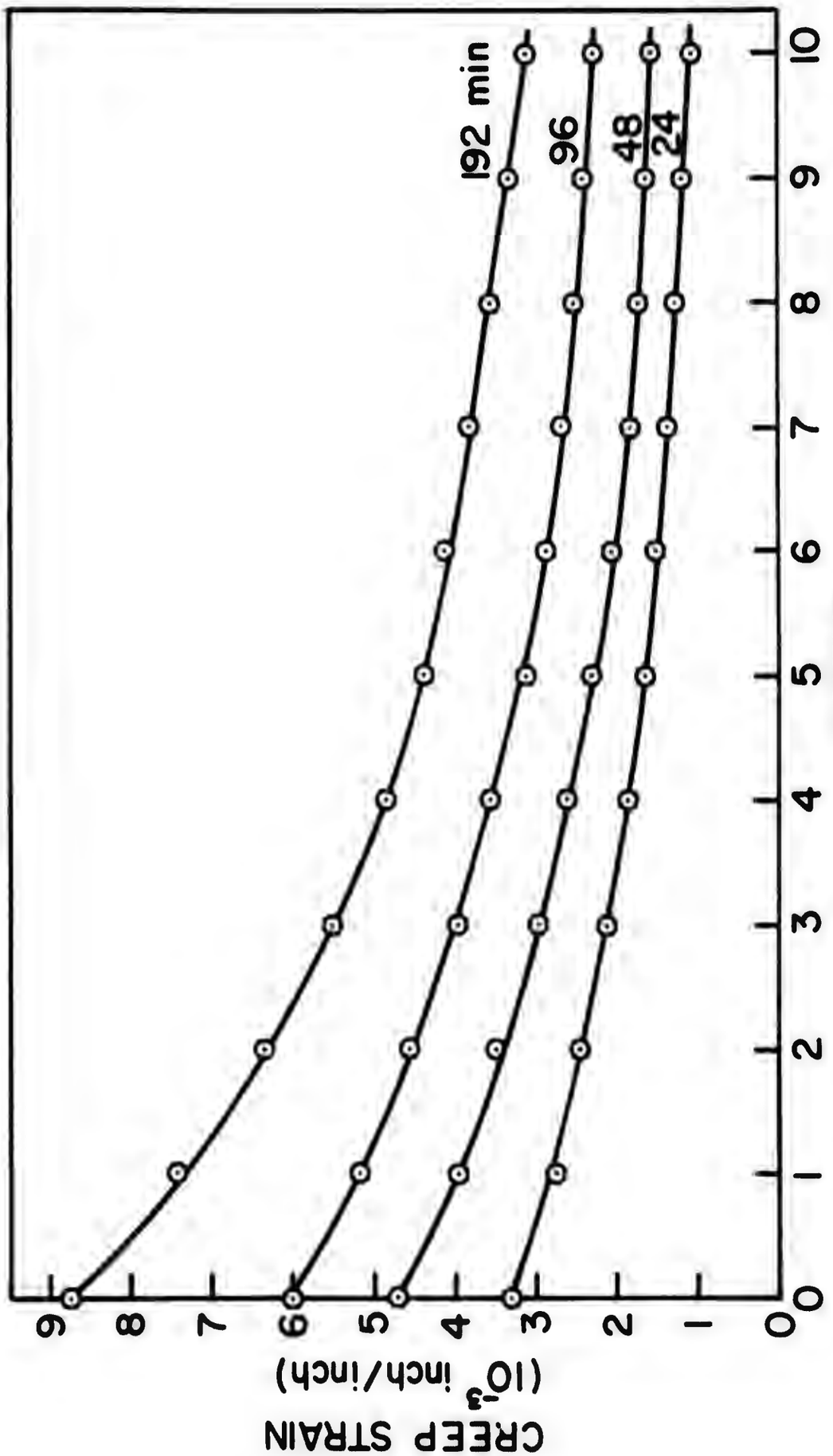

Fig. 11 Creep strain data.

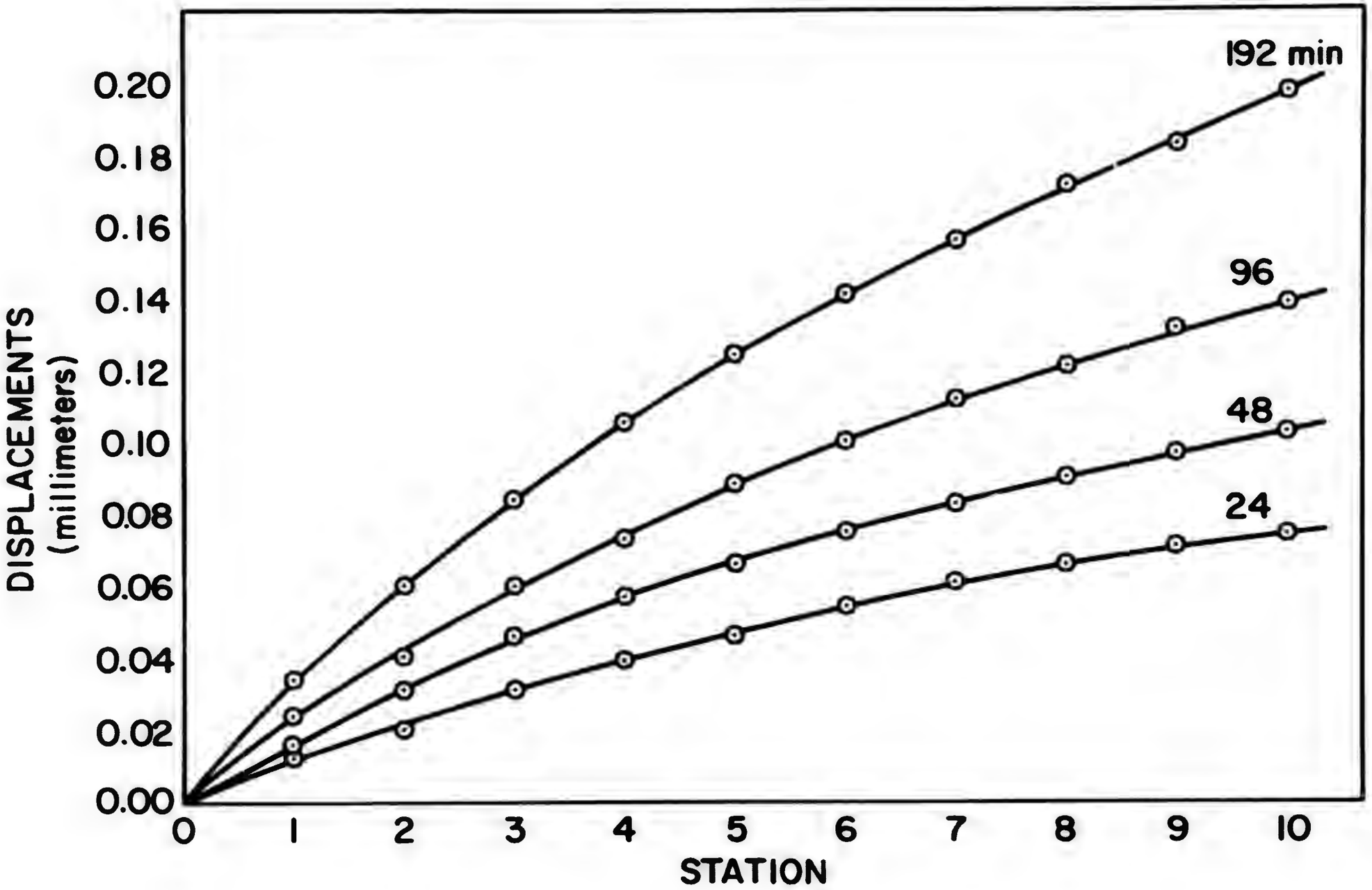

Fig. 10 Displacement data.

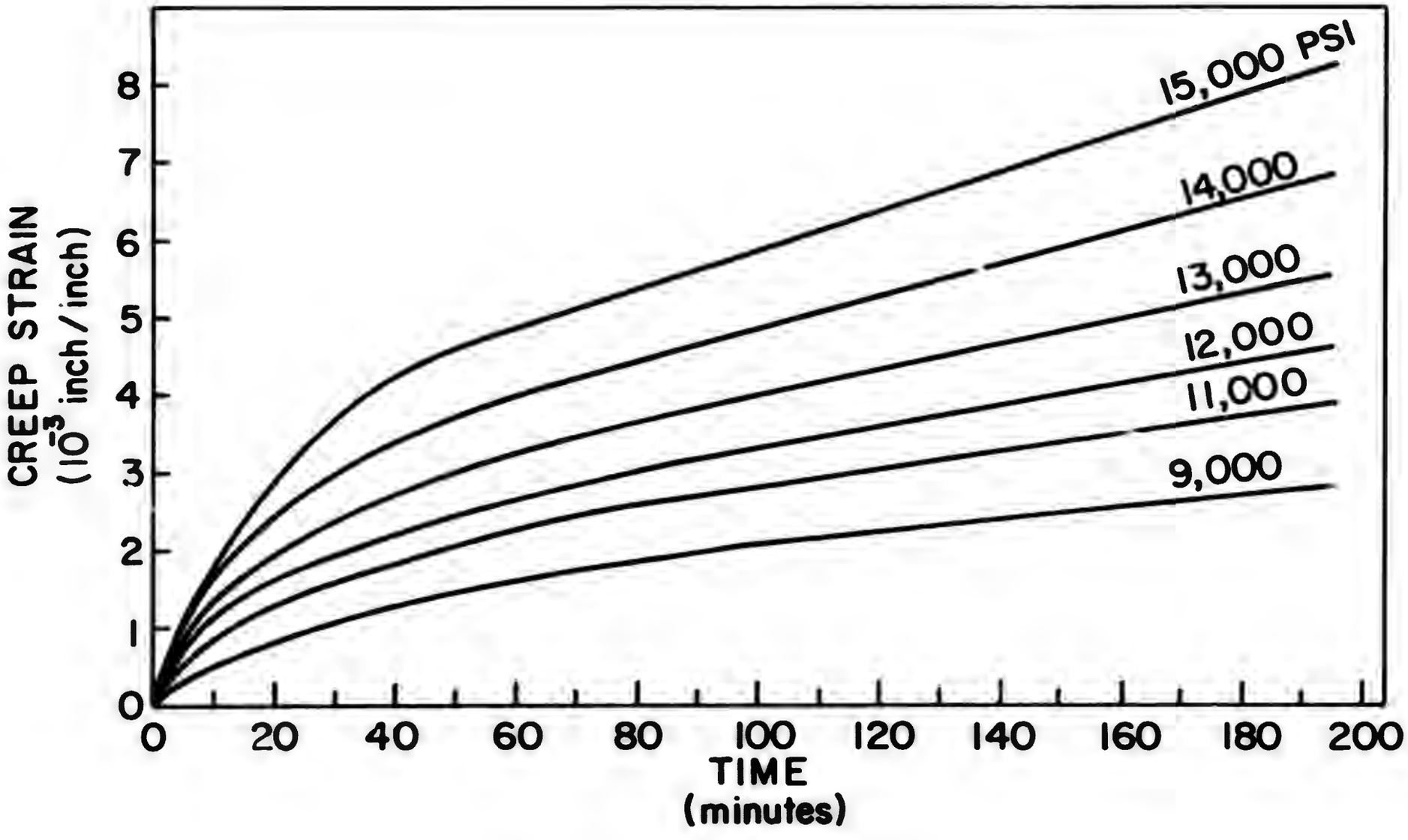

Figl 13 Creep strain vs. time data.

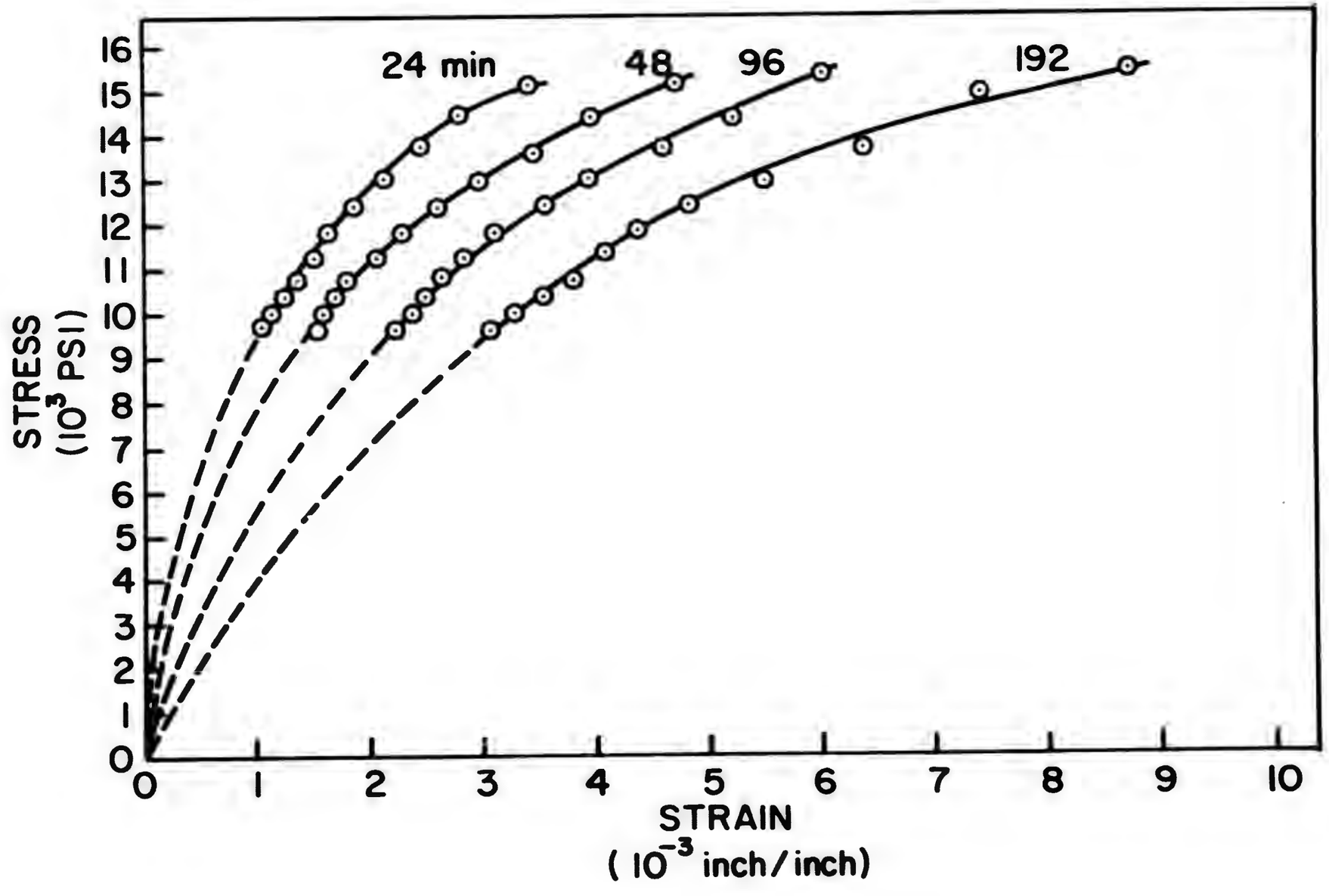

Fig. 12 Isochronous stress-strain curves.

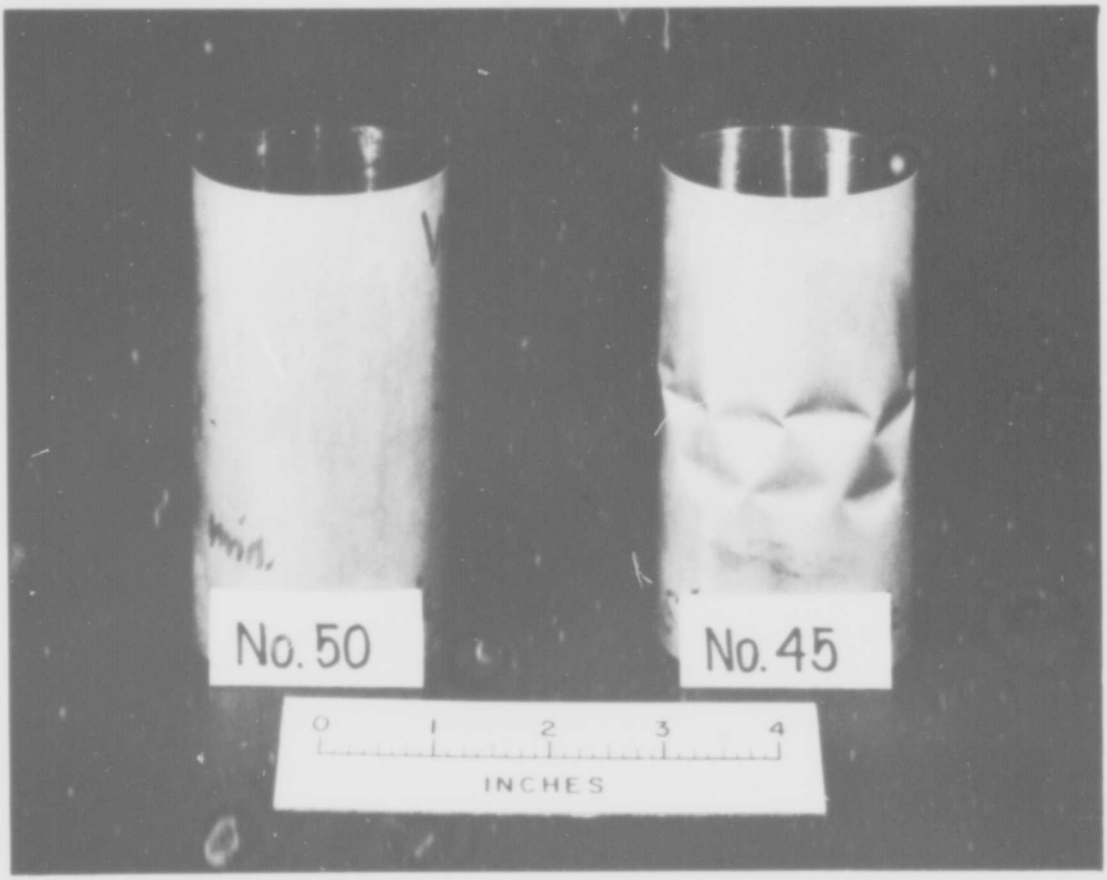

Fig. 14 Shell specimens, before and after testing.

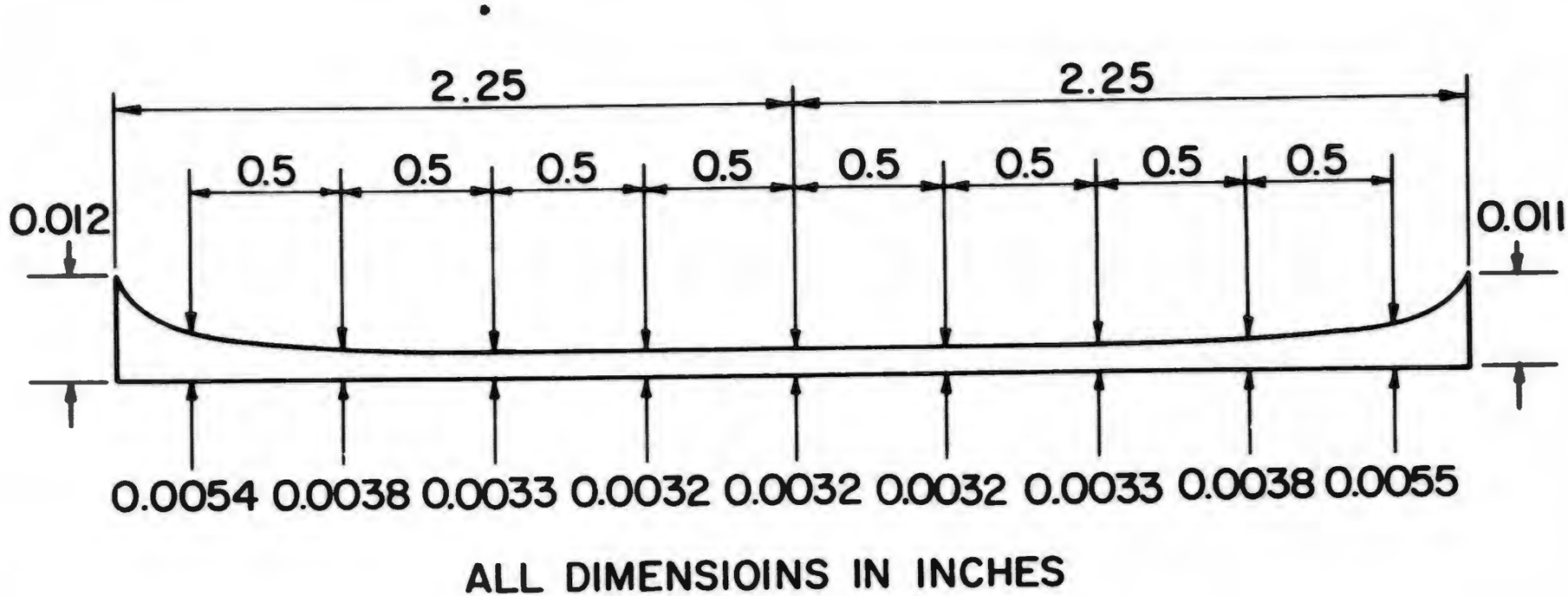

Fig. 15 Typical section of cylinder wall.

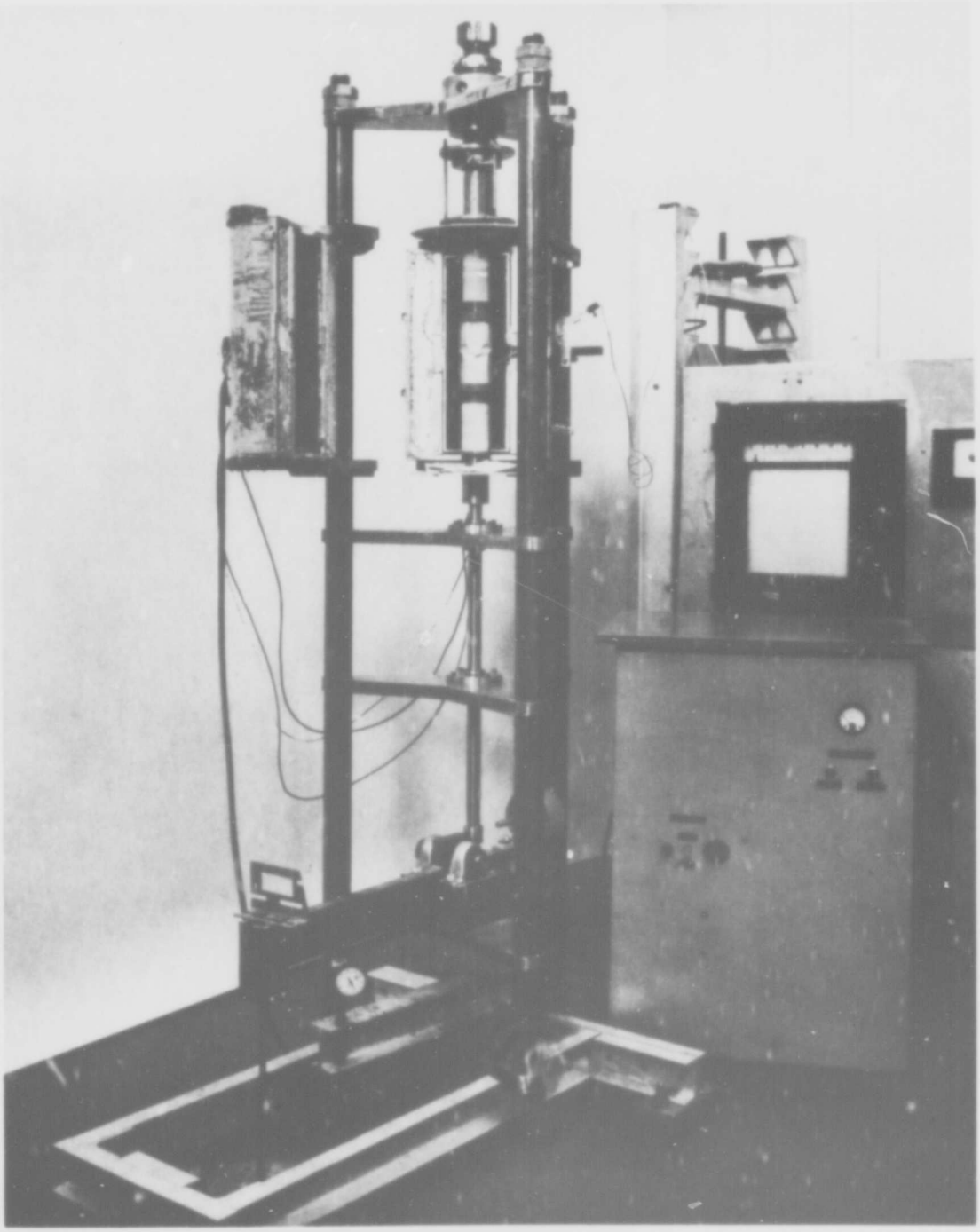

Fig. 16 Creep buckling test unit.

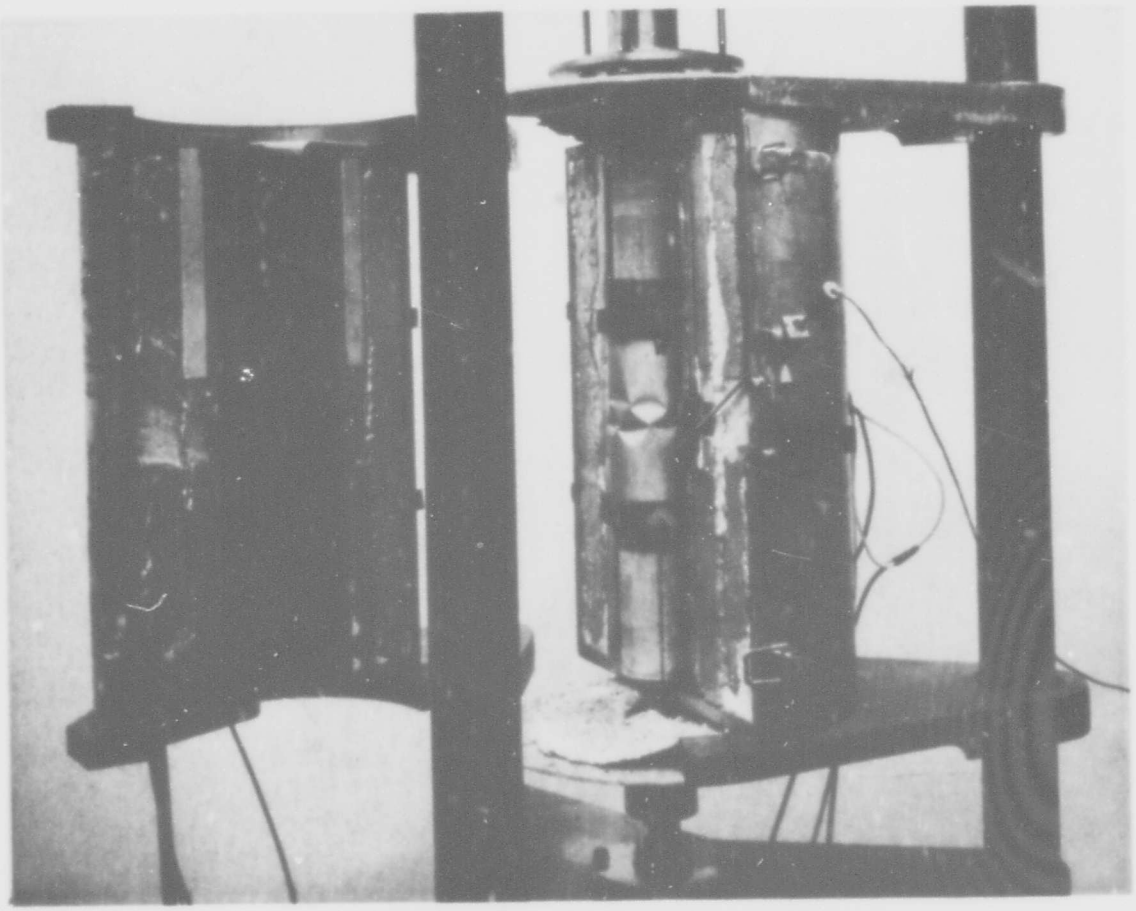

Fig. 17 Furnace of test unit.

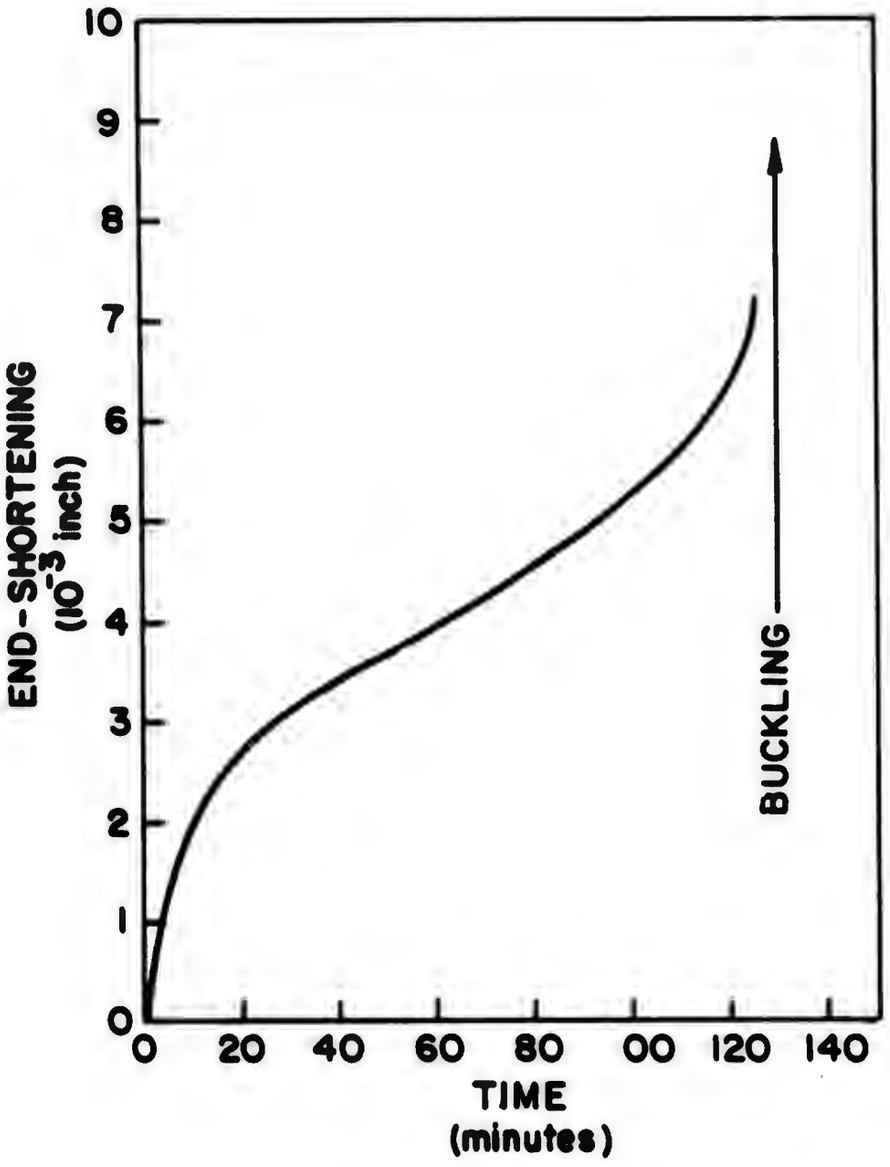

Fig. 18 End-shortening history.

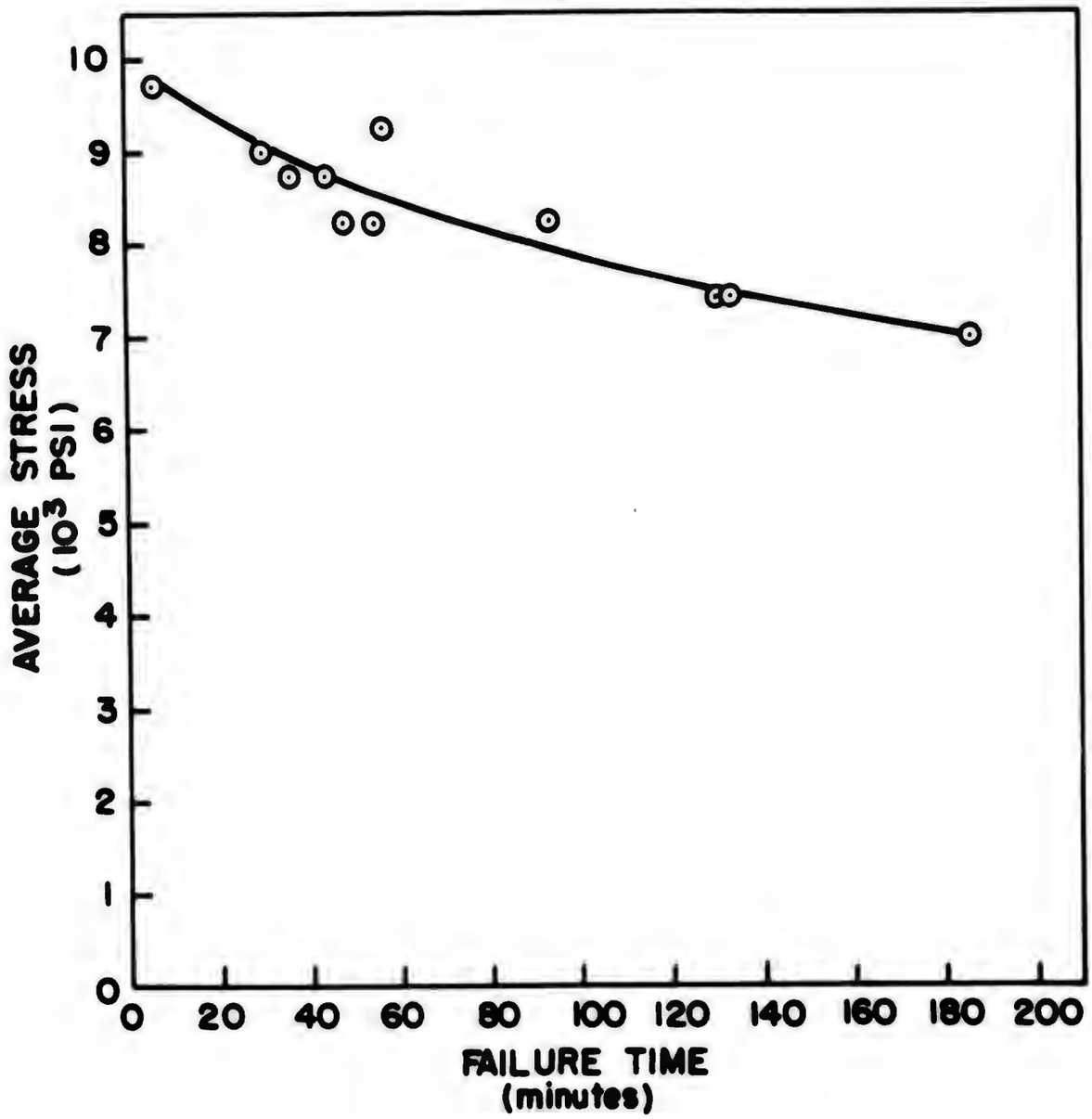

Fig. 19 Average stress versus time to buckling.